OPEN ACCESS
OPUS AUGSBURG

Universität Augsburg
Universitätsbibliothek

Mechanical properties and damage evolution of a structural sheet molding compound based on a novel two step curing resin system

Anna Trauth, M. Bondy, Kay A. Weidenmann, W. Altenhof

Angaben zur Veröffentlichung / Publication details:

Trauth, Anna, M. Bondy, Kay A. Weidenmann, and W. Altenhof. 2018. "Mechanical properties and damage evolution of a structural sheet molding compound based on a novel two step curing resin system." *Materials and Design* 143: 224–37. https://doi.org/10.1016/j.matdes.2018.02.002.

Nutzungsbedingungen / Terms of use: **CC BY-NC-ND 4.0**

Dieses Dokument wird unter folgenden Bedingungen zur Verfügung gestellt: / This document is made available under these conditions:
CC-BY-NC-ND 4.0: Creative Commons: Namensnennung - Nicht kommerziell - Keine Bearbeitung
Weitere Informationen finden Sie unter: / For more information see:
https://creativecommons.org/licenses/by-nc-nd/4.0/deed.de

Mechanical properties and damage evolution of a structural sheet molding compound based on a novel two step curing resin system

A. Trauth [a], M. Bondy [b], K.A. Weidenmann [a], W. Altenhof [b,*]

[a] *Karlsruhe Institute of Technology, Institute for Applied Materials, Karlsruhe, Germany*
[b] *University of Windsor, Department of Mechanical, Automotive and Materials Engineering, Windsor, Canada*

* Corresponding author.
E-mail address: altenh1@uwindsor.ca (W. Altenhof).

1. Introduction

Due to their outstanding specific strength and stiffness combined with a cost efficient manufacturing process, sheet molding compound (SMC) has become a very attractive material for the automotive industry, which represents an important and growing field of application for polymer composites. In contrast to SMC developed in the 1960s, advanced and structural SMC, developed in the last few years has to fulfill higher demands regarding mechanical properties, as an example, the requirement to be used in structural components prone to crash loads. Structural glass fiber SMC components have recently been implemented into different vehicle concepts, for example the Dodge Viper [1] or the Mercedes S-Class [2]. With the BMW 7 series, structural carbon fiber SMC was also successfully implemented in a production vehicle in the form of the cross member/trunk cover, molded from an epoxy sheet molding compound [3]. The implementation of SMC components into vehicle concepts has prompted the above-mentioned need to understand the influence of loading rate and manufacturing induced anisotropy on the structural behavior of SMC to offer appropriate material data for simulation. Impact and puncture loadings are important to consider while designing novel materials for the automotive industry since low-energy impact damages may arise frequently due to low velocity collisions, dropped hand tools or flying stones on the roads.

The investigation of SMC with advanced resin formulations already showed their superior mechanical properties and the potential to consider this material class for structural components.

In general, approaches focus on an increase of the fiber volume content by decreasing the amount of fillers [4] or by reducing the density of the material by adding hollow glass sphere to the resin, for example [5]. Another promising approach to enhance mechanical material properties is a substitution of the glass by carbon fibers [6].

However, taken loading rate dependence into account, only a few studies have already investigated the structural and material behavior of SMC exposed to higher loading rates.

A first attempt to investigate impact properties of SMC by Kau [7] showed that the thickness of the specimen as well as the individual constituents, thus fiber and matrix type, influence the impact response of glass fiber SMC for a puncture velocity of 2.5 m s^{-1} in a distinct way. The influence of matrix type on impact properties of SMC was also stated by Sadasivam et al. [8]. Lee et al. pointed out that failure mechanisms strongly depend on striker type and energy absorption capacity of SMC increased with increasing specimen thickness for puncture velocities from 1.4 m s^{-1} to 4.75 m s^{-1} [9]. Dear et al. also indicated that the in-plane modulus is the dominant mechanical property of SMC, if impact loadings are present. Additionally, the observed SMC materials exhibited hidden through-thickness damage long before damage was visible at the outer surface [10]. Chaturvedi et al. concluded, that the impactor size and mass significantly effects the size and growth of damage of SMC exposed to puncture loadings [11]. These aforementioned studies all focused on impact properties of standard SMC materials. No attention was paid to the rate dependence of the SMC material.

To the best of the author's knowledge, literature on loading rate dependence of glass, but most especially on carbon fiber SMC exposed to puncture loading, is barely available.

Taking recent research results into consideration, this contribution presents novel aspects in the field of SMC. First of all, the two step curing resin was successfully implemented to manufacture glass and carbon SMC without fillers. This enables to further increase the fiber volume content and thus mechanical material properties combined with lower densities as for filled resin systems. Additionally, the novel, two step curing resin system also enables to manufacture continuously carbon fiber reinforced sheet molding compounds in an adapted SMC process [12]. To combine the advantages of continuously and discontinuously fiber reinforced materials, different concepts of hybrid sheet molding compounds were presented within the last few years. One approach by Fette et al. focuses on components of discontinuous SMC with a local reinforcement due to continuous prepregs [13–15]. The same approach was also followed by Wulfsberg et al. [16] and Corbridge et al. [17] the last few years. This approach has a decisive disadvantage, since manufacturing and material costs of continuous carbon fiber prepregs are very high. Gortner et al. presented an alternative to locally reinforce SMC with dry textile preforms. However, impregnation of the dry textile during molding is a critical factor for mechanical material properties [18].

The novel two step curing resin system presented within this study, allows to manufacture discontinuously as well as continuously fiber reinforced semi-finished sheets on a standard SMC processing line in an economic way [12]. These two components can be combined in a one shot process during compression molding with the use of the same resin system for both components enabling a chemically strong bond. To the authors knowledge, this approach is unique in the field of hybrid continuous-discontinuous sheet molding compounds.

To better understand the mechanical behavior and to provide data for material simulation a profound understanding of both constituents, thus the continuously and the discontinuously fiber reinforced SMC are necessary. This contribution is a first step towards a deeper understanding of the mechanical properties of the discontinuous glass and carbon fiber SMC based on the novel two step curing resin system. In addition, this contribution focuses in detail on puncture properties and damage evolution of glass and carbon fiber unfilled advanced SMC at different loading rates for the first time.

2. Materials

2.1. Material manufacturing

The discontinuous structural SMC considered within this study was based on an unsaturated polyester-polyurethane (UPPH) resin system by Aliancys, Schaffhausen, Switzerland. The particularity of this resin system is a two step curing process. First, the resin is thickened by the help of di-isocyanate which leads to a chemical stable and highly viscous B-stage due to chain extension. In a second curing step, during molding at elevated temperatures, a radical polymerization is performed, which allows for fast curing and chemical bonding. This two step curing process enables control of the paste's viscosity throughout the whole process chain and to also adopt it to improve impregnation of glass or carbon fibers [12]. No fillers were added to the resin system. The exact compositions of the resin system for the glass and carbon fiber SMC are listed in Table 1. The semi-finished sheets were manufactured using a flat conveyor plant type HM-LB-800 by Schmidt & Heinzmann (Bruchsal, Germany) at the Fraunhofer ICT in Pfinztal, Germany. After maturation the semi-finished SMC sheets were cut into plies, stacked and compression molded into plaques at approximately 150 °C, 1600 kN, and 122 s mold closing time. The charge was either placed in the middle of the rectangular mold, with a coverage of 40 ± 1%, to ensure flow in two directions (2D) or at one side of the mold, leading to a material flow only in one direction (1D) (Fig. 1). The dimensions of the compression molded plaques were 458 mm by 458 mm with a nominal thickness of 3 ± 0.2 mm. Table 2 lists the dimension of flow, thickness of the plaques, fiber volume content, and fiber length of the glass and carbon fiber sheets considered within this study. The difference in fiber volume content results due to conditions of manufacturing. Unpublished preliminary work pointed out that carbon fiber SMC with lower fiber volume contents led to unsatisfying mechanical material properties. The fiber volume content of the glass fiber SMC could not be significantly increased to ensure a sufficient impregnation on the conveyor belt. The authors aimed to realize the same density of the two materials, to obtain structures with the same weight to realize a level of comparability.

2.2. Specimen preparation

Specimens for experimental investigation were extracted by water jet cutting by SNZ Schneidbetrieb GmbH, Mühlacker, Germany. Tensile

Table 1
Individual resin components and fiber type of investigated glass and carbon fiber SMC.

Component		Glass fiber SMC (GF SMC)	Carbon fiber SMC (CF SMC)	Supplier
Resin		Daron ZW 14141	Daron ZW 14142	Aliancys
Additives	Release agent	BYK 9085	BYK 9085	BYK
	Inhibitor	pBQ	pBQ	Fraunhofer ICT
	De-airing	BYK A 530	BYK A 530	BYK
	Impregnation additive		BYK 9076	BYK
Peroxide		Trigonox 117	Trigonox 117	Akzonobel
Thickener	Isocyanate	Lupranat M20R	Lupranat M20R	BASF
Fiber		MultiStar 272	Panex35	Johns Manville Zoltek

specimens featured a length of 200 mm and a width of 15 mm. The flat, square specimens for puncture testing featured a section of 140 mm by 140 mm according to ISO 6603-2. To evaluate the influence of material flow during compression molding, specimens were extracted from the charge as well as the flow region as identified in Fig. 1. In addition, tensile specimens were extracted in 0° and 90°.

3. Methodology

3.1. Tensile testing

To evaluate the Young's modulus and tensile strength of the considered materials quasi-static tensile tests were carried out on a ZwickRoell Zmart. Pro universal testing machine with a load cell capacity of 200 kN. The nominal testing velocity was 1.8 mm min^{-1}. The specimens were clamped at a distance of 100 mm. The deflection was measured using an extensometer and a gage length of 70 mm. The Young's modulus was determined according to ASTM E1111 with a least squares method in the strain range from 0.05% to 0.25%. Tensile properties were based on eight specimens for each material configuration extracted from charge and flow region. A specimen was only considered for evaluation if failure occurred in the gage section.

3.2. Quasi-static puncture testing

Quasi-static puncture tests were performed on a MTS Criterion Model 45 electromechanical load frame. A lubricated (PC Waylube 68) hemispherical striker, having a diameter of 20 mm, punctured the rectangular specimen perpendicular to its surface with a nominally uniform velocity of 2.6 mm min^{-1} (approx. 4.4 10^{-5} s^{-1}) up to a defined maximum deflection of 16 mm. A custom made fixture allowed for clamping of the flat, square specimen mechanically under a metallic plate to provide a circular puncture area with a diameter of 100 mm. This clamping leads to a complex 2D stress state combining multiaxial tension and bending. The contact of the striker furthermore leads to a localized 3D stress state. The resulting force was recorded by a load cell with a capacity of 150 kN. Deflection between the striker and the specimen support, starting from first contact between the striker and the specimen, was measured by the crosshead displacement of the MTS load frame. The test rig was designed such that a front surface mirror allowed for video capturing during the test to track damage evolution. For this purpose a Point Grey Research Grasshopper GRAS-50S5M 5.0 MP monochrome camera with 35 mm CM120 Schneider-Kreuznach lens was placed at one side of the fixture underneath the specimen. One frame per second was captured throughout the quasi-static loading up to the maximum deflection. An external light source and an inclined mirror beneath the specimen ensured sufficient illumination. Synchronization between the load frame and camera was established with the Correlated Solutions VIC-Snap transistor to transistor logic (TTL) interface and a signal from the load frame at a user defined digital output connected to a National Instruments (NI) USB 6221 BNC data acquisition device. Six specimens of each configuration were considered for testing. For the charge region of 1D flow carbon fiber SMC only 5 specimens were considered for testing.

3.3. Dynamic puncture testing

Low-velocity impact tests, in the following named dynamic puncture tests, were conducted with a custom drop tower modified to carry out ISO 6603-2 instrumented impact testing. The impacting unit consisted of three different parts, namely the crosshead, a shaft including the load cell and a hemispherical tip with a diameter of 20 mm. During the test, the drop weight was released at a defined height and traversed down guide rails to impact the specimen at its center, perpendicular to the surface, at a nominal uniform velocity of 4.4 ± 0.2 m s^{-1}. The flat, square specimens were mechanically clamped under a metal plate to provide a circular impact area with a diameter of 100 mm, consistent to the quasi-static puncture testing. Since external forces, which are applied to the specimen, are limited to the striker and the clamping system, the only work done to the specimen is by the striker, as there is

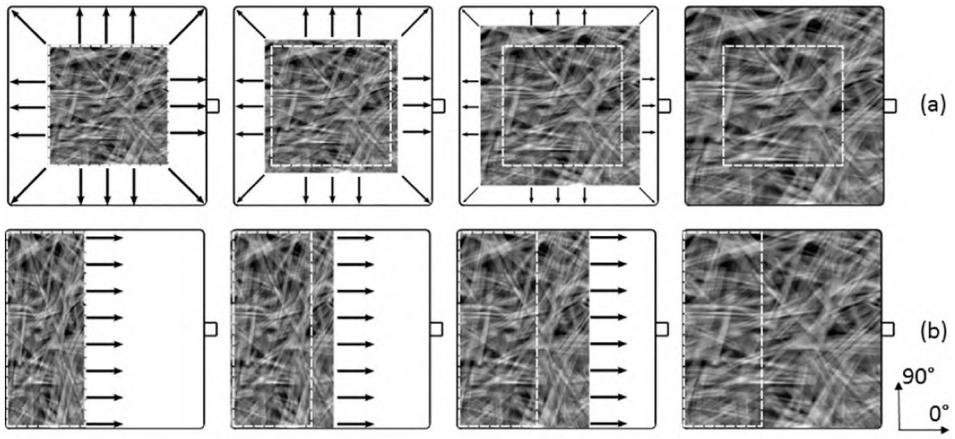

Fig. 1. Schematic representation of 2D (a) and 1D (b) flow SMC semi-finished sheets during compression molding. Dashed line indicates initial charge.

Table 2
Material properties of glass and carbon fiber SMC plaques and puncture specimens.

	Glass fiber SMC (GF SMC)	Carbon fiber SMC (CF SMC)	
Flow (dimension)	2	2	1
Fiber type	Glass	Carbon	Carbon
Nominal fiber volume content (%)	22	42	42
Fiber length (mm)	25.4	25.4	25.4
Theoretical density (g/cm^3)	1.44	1.43	1.43
Average thickness (mm) of specimens considered for puncture loading	3.1	2.9	3.1
Coefficient of variation (%) of thickness of specimens considered for puncture loading	1.56	2.09	4.03

no deflection at the clamping ring. Due to the large mass of the drop tower carriage (approximately 60 kg), the change in carriage velocity resulting from energy absorption by the specimen is negligible. The test rig was designed such that a front surface mirror allowed for high speed photography with a Photron SA4 camera placed on the floor in front of the drop tower. The resulting crosshead deflection and forces were measured with an Acuity laser displacement transducer with a sensitivity of 30 mm/V and a Dytran Model 1050 Integrated Electronic Piezoelectric (IEPE) load cell, respectively. The load cell was integrated in the shaft of the striker, thus ensuring measurement of the impact load very close to the location of contact between the nose and SMC specimen. A custom LabVIEW program was developed to acquire force-deflection data and appropriately trigger the high speed camera and synchronize transducer data acquisition with the high speed photograph acquisition. Force-time data was acquired at 50 kHz with a 24 bit resolution National Instrument (NI) 9233 IEPE data acquisition module in an NI CompactDAQ chassis. Deflection-time data was acquired at 50 kHz with a 16 bit NI 9205 analog input module. The high speed camera was triggered with a transistor to transistor logic (TTL) signal from an NI 9401 digital input/output module. Images were captured for a total duration of 10 ms. For glass fiber SMC specimens, images were captured with a frame rate of 13,500 frames per second, a shutter speed of 1/25000 s and a resolution of 512 by 512 pixel^2. For carbon fiber SMC specimens images were captured with a frame rate of 45,000 frames per second, a shutter speed of 1/71000 s and a resolution of 256 by 256 pixel^2. Six specimens of each configuration were considered for testing.

3.4. Data processing

The raw force-deflection data captured by the laser displacement transducer and load cell were processed within MATLAB® 2015. The time at which contact between the striker and specimen occurred was estimated by finding the mean and standard deviation of the load prior to contact. Any initial offset was removed and the initiation of contact was identified by searching for the first instant at which the load was greater than 6 standard deviations. Contact was estimated to initiate one data point prior to this event. The deflection refers to the position of the striker, which is defined as having a value of zero at the first contact with the surface of the specimen. A four pole Butterworth filter (two pole filter with forward and reverse passes) was applied to the load-time data with a channel frequency class (CFC) of 600 (approximately 1000 Hz cutoff) consistent with SAE standard J211. Quasi-static force-time data was not filtered. Energy during puncture was computed by integration the force-deflection response with the trapezoid method. To evaluate the puncture properties of the SMC materials, the maximum force as well as the absorbed energy, further referred to as puncture energy E_p, for the two considered loading rates were taken into account. In this investigation the puncture energy of the specimen during quasi-static or dynamic loading equals

$$E_P = \int_0^{x_p} F dx \tag{1}$$

with the force F and the deflection x. In an effort to eliminate frictional effects between striker and punctured surface, according to ISO 6603-2, puncture energy, E_p, is calculated according to Equation (1) up to the puncture deflection (x_p). This is the deflection referring to the point when measured load is half of the precedent maximum load occurred during puncture. Fig. 2 shows the unfiltered and filtered force-deflection response for the same specimen. It also highlights the mean value and standard deviation of the filtered and unfiltered maximum force and resulting puncture energy for the glass fiber SMC specimens. Considering the maximum force, filtering of the data leads to slightly lower values (Fig. 2b). The filtering does not influence the calculated puncture energy (Fig. 2d). In the following, filtered force is plotted in the diagrams. The filtered force-deflection response was also considered to calculate the puncture energy of the specimen. High speed imagery was processed with ImageJ.

4. Results

4.1. Quasi-static tensile properties

The Young's modulus of the glass fiber SMC (Fig. 3 a) ranges between 11 GPa and 12.4 GPa. It shows a slight increase for flow region specimens compared to charge region specimens. However, due to the high scatter of experimental results of flow region specimens (Coefficient of variation $C_V = 13\%$ and 9.4% for 0° and 90°), this increase is not significant. Tensile strength of the 2D glass fiber SMC (Fig. 3b) also shows a slight increase for flow region specimens compared to charge region specimens (from 143.4 MPa to 167.4 MPa for 0° specimens and from 146.3 MPa to154.2 MPa for 90° specimens). The scatter of tensile strength of flow region specimens ($C_V = 12.9\%$ (0°) and $C_V = 12.7\%$ (90°)) is slightly higher than the scatter of tensile strength of charge region specimens ($C_V = 9.9\%$ (0°) and $C_V = 7.2\%$ (90°)). Due to the material flow the fibers tend to orientate in flow direction explaining the slight increase in stiffness and strength of the flow region specimens. Since a 2D flow was realized, the increase was noted for both considered directions. The observed differences in stiffness and strength are only tendencies and not significant due to the high scatter of the measured mechanical properties. The average strain at failure equals 1.7%. Exposed to uniaxial tension the glass fiber SMC failed due to sudden fracture.

The 2D flow carbon fiber SMC shows no significant difference in stiffness and the average Young's modulus of the four different configurations ranges between 26 GPa and 29.6 GPa with a coefficient of variation of $C_V = 10.9\%$ to $C_V = 21.7\%$ (Fig. 4a). The 1D flow carbon fiber SMC leads to highly oriented fibers and a significant difference in stiffness for 0° and 90° specimens. The average stiffness (coefficient of variation) in flow direction is 33.5 GPa ($C_V = 13.7\%$) for charge and 37.4 GPa ($C_V = 10.8\%$) for flow region specimens. Specimens extracted perpendicular to the flow direction show a significantly lower stiffness with an average Young's modulus of 18.1 GPa ($C_V = 12.9\%$) for charge and 19.3 GPa ($C_V = 33.2\%$) for flow region specimens. The tensile strength shows the same trend (Fig. 4b). With an average strain at failure of 0.43% for 1D and 0.46% for 2D flow, carbon fiber SMC behaves notably more brittle than glass fiber SMC. Exposed to uniaxial tension the 1D and 2D carbon fiber SMC failed due to sudden fracture.

4.2. Puncture properties and rate sensitivity of glass fiber SMC

4.2.1. Influence of flow during compression molding on puncture properties

There is no significant difference for charge and flow region specimens considering quasi-static force-deflection response and no significant trend in terms of puncture energy was noted considering specimen location (Fig. 5a and c). Punctured glass fiber SMC specimens, loaded in a dynamic condition and extracted from flow region, showed a slightly higher scatter in resulting force-deflection and energy-deflection response than charge region specimens (Fig. 5b and d).

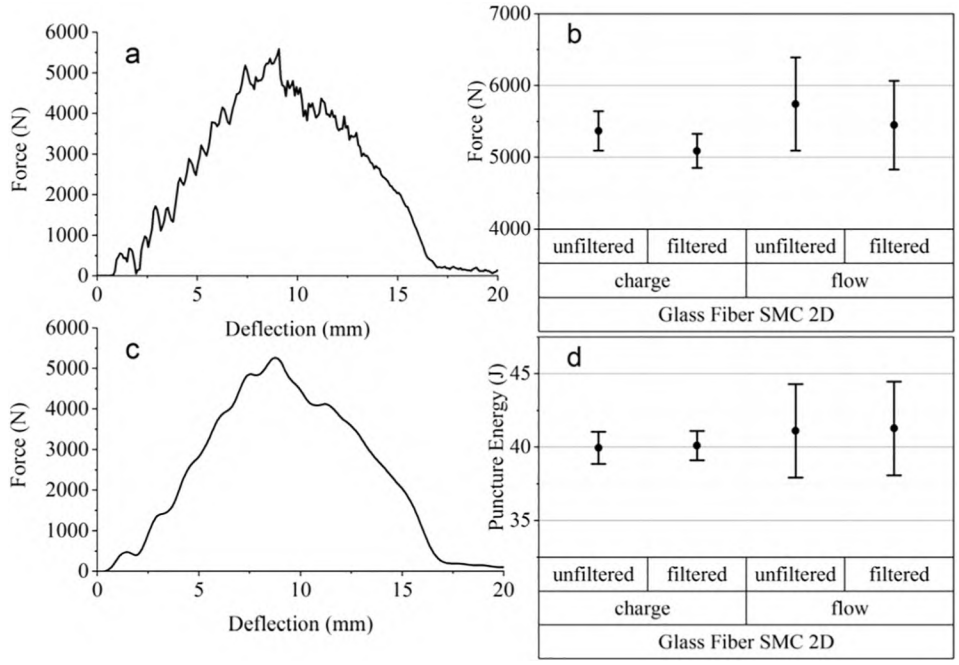

Fig. 2. Unfiltered (a) and filtered (c) force-deflection response and resulting values of maximum force (b) and puncture energy (d) for 2D glass fiber SMC punctured in a dynamic manner.

4.2.2. Rate sensitivity of glass fiber SMC exposed to puncture loadings

To evaluate the loading rate dependence of glass fiber SMC, the maximum force and puncture energy resulting from puncture penetration at the two different loading rates are depicted in Fig. 6.

With an increase in loading rate, maximum force during puncture increases 65% for specimens extracted from the charge region and 73% for flow region specimens. This increase in maximum force also leads to an increase in absorbed energy for puncture at higher loading rates and the 2D glass fiber SMC shows an increase in puncture energy of 67% for charge region specimens and 64% for flow region specimens. The orientation of the fibers during compression molding leads to an increase in scatter of the observed puncture properties for flow region specimens, independent from loading rate.

4.2.3. Damage evolution of glass fiber SMC exposed to puncture loadings

To investigate the damage evolution and energy absorption mechanisms of punctured glass fiber SMC, Fig. 7 shows the force-deflection as well as energy-deflection responses resulting from quasi-static and dynamic puncture. The upper and lower case letters indicate significant points of the force-deflection evolution. The corresponding images at these levels of deflection are shown in Figs. 8 and 9. Considering the force-deflection evolution resulting from quasi-static puncture of glass

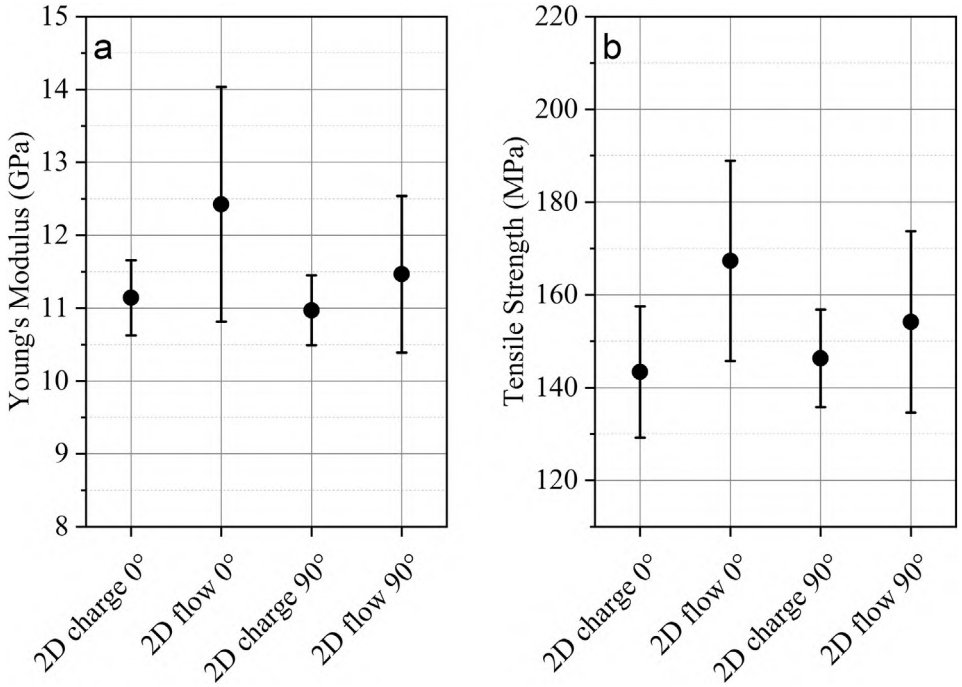

Fig. 3. Young's Modulus (a) and tensile strength (b) of 2D glass fiber SMC.

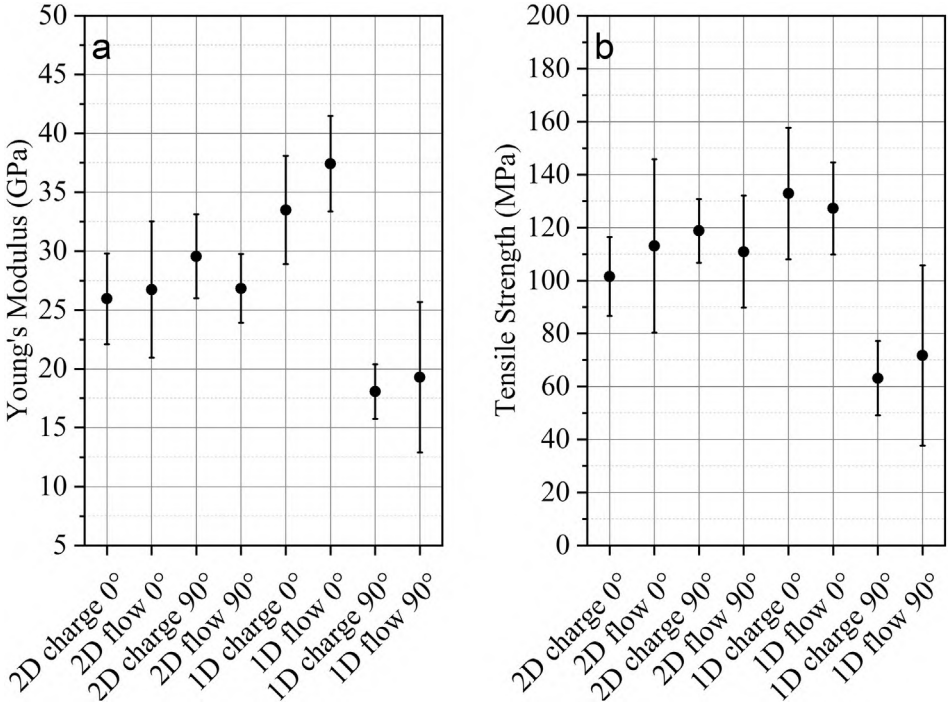

Fig. 4. Young's Modulus (a) and tensile strength (b) of 1D and 2D carbon fiber SMC.

fiber SMC the first part of the force-deflection response up to point (d) shows a bi-linear evolution. This evolution is marked by a stiffness decrease in point (b), resulting from partial failure of the specimen at the lower surface due to the formation and growths of numerous cracks.

This network is dominated by two major cracks, forming a cross-like shape. Up to maximum load, the crack network growths in number and size of the precedent formed cracks. After point (d) the force significantly reduces as a result of failure of the specimen. Following this, the nose of the striker further pushes through the failed material which bends outwards (point (e) through (f)). A decrease in the force-deflection response (points (f) through (h)) occurs until the specimen is fully punctured (point (i)). Then the shaft of the striker slides along the punctured specimen. In this phase, energy is dissipated due to frictional sliding between the specimen and shaft of the striker. Energy absorption is based during the whole penetration event on the formation and growth of cracks, especially on the lower surface of the specimen with a significant increase beginning from point (b) up to final failure of the specimen. Considering dynamic penetration, the force-deflection response also shows an increase in force up to its maximum value in point (C). The small force drops result due to the testing setup and wave reflections and do not reflect material behavior since the location of these load drops are reproducible for different specimens

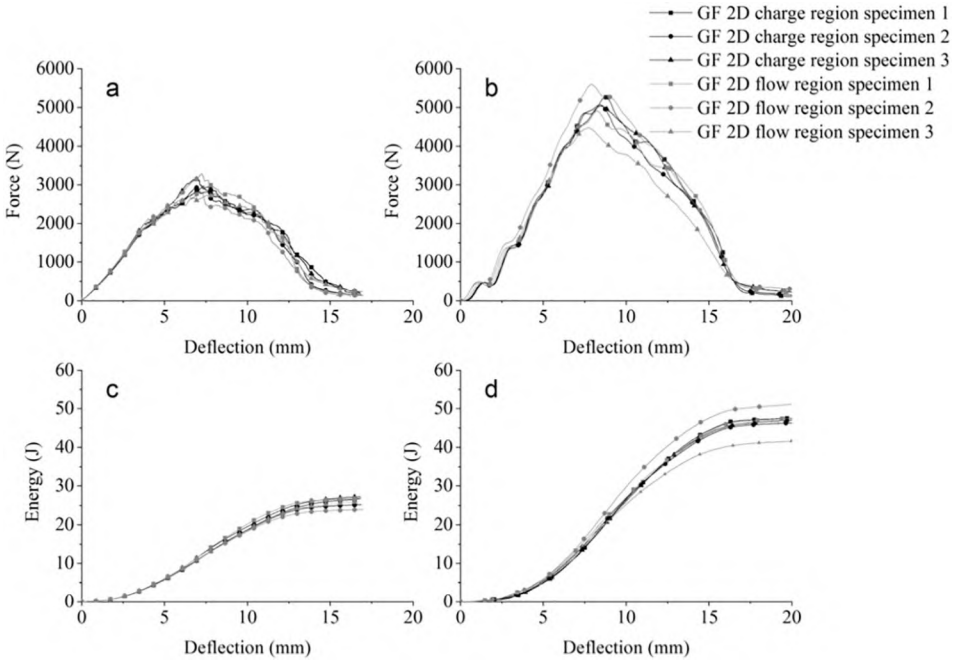

Fig. 5. Quasi-static (a) and dynamic (b) force-deflection and quasi-static (c) and dynamic (d) energy-deflection response resulting from puncture of 2D glass fiber.

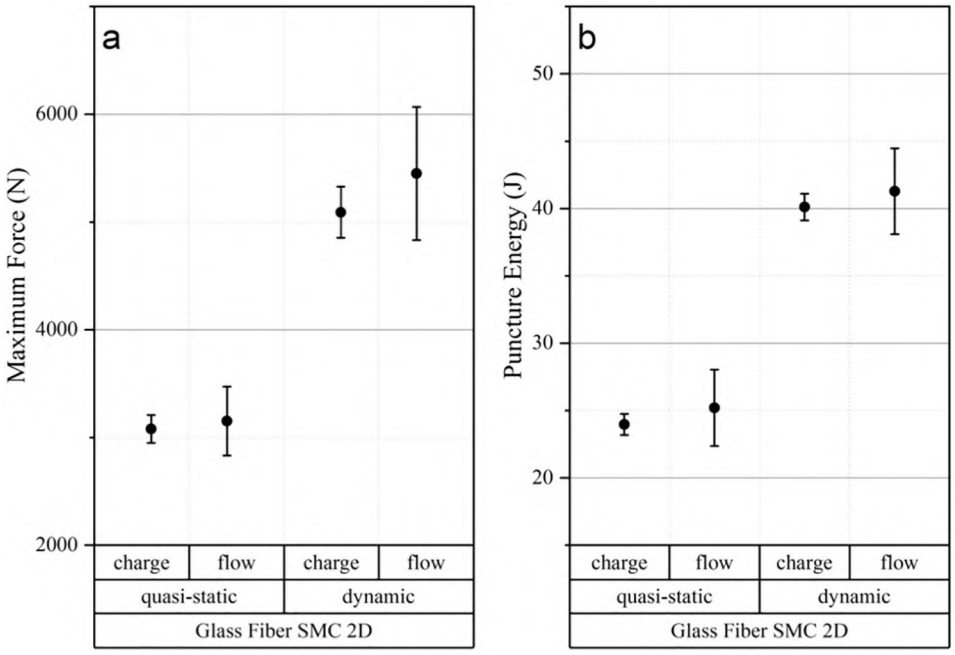

Fig. 6. Maximum force (a) and puncture energy (b) resulting from quasi-static and dynamic puncture of 2D glass fiber SMC.

(see Fig. 5(b)). The slope of the force-deflection response tends to increase from first contact to the maximum force. This effect can possibly be explained by membrane effects. First visible damage occurs at maximum load (C), thus later than for specimens, punctured in a quasi-static manner. After reaching maximum force, load drops due to penetration of the striker through the specimen, comparable to the evolution for a quasi-static loading. As far as energy absorption is considered, significant increase in energy absorption is linked to higher deflections for dynamic puncture. This matches very well with the retarded appearance of visible damage at the lower surface of the specimen for higher loading rates.

4.3. Puncture properties and rate sensitivity of carbon fiber SMC

4.3.1. Influence of flow during compression molding on puncture properties

For 2D flow carbon fiber specimens flow of the material does not significantly increase maximum force and puncture energy, but the specimens extracted from the flow region tend to show higher scatter in their force-deflection as well as energy-deflection response (Fig. 10a and b). 1D carbon fiber SMC flow region specimens show lower maximum forces and energy absorption capabilities compared to charge region specimens (Fig. 11). For both manufacturing routes the carbon fiber SMC specimens show a higher scatter in puncture properties compared to the glass fiber SMC specimens. This is due to the high number of carbon fibers in one fiber bundle and the spreading of these bundles during manufacturing, leading to a highly anisotropic microstructure of the material. Since puncture results in a very localized loading, the response of the specimen is mostly determined by the local fiber distribution and orientation at the point of contact, which is more heterogeneous for the carbon than for the glass fiber SMC. Carbon fiber SMC also tends to behave more brittle than glass fibers, leading to lower observed deflections at maximum load as well as puncture deflection for both, quasi-static and dynamic, loading.

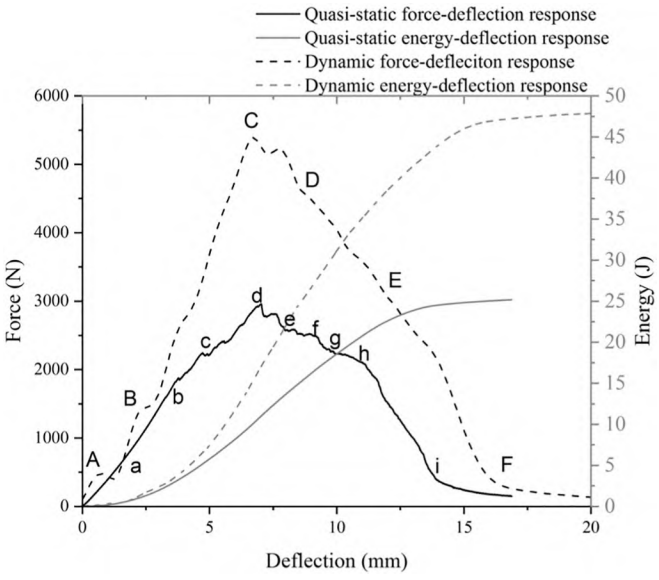

Fig. 7. Force-deflection and energy-deflection responses resulting from quasi-static and dynamic puncture of 2D glass fiber SMC.

4.3.2. Rate sensitivity of carbon fiber SMC exposed to puncture loadings

In general, 2D carbon fiber SMC shows lower maximum force and puncture energy compared to 1D carbon fiber SMC. There is no significant difference in energy absorption capability depending on loading rate neither for 2D carbon fiber SMC nor for the 1D carbon fiber SMC. Only flow region specimens of 1D flow carbon fiber SMC loaded in a dynamic manner show a decrease in maximum force and puncture energy (Fig. 12).

4.3.3. Damage evolution of carbon fiber SMC exposed to puncture loadings

Considering quasi-static as well as dynamic puncture, the force-deflection response of the carbon fiber SMC specimens can be compared in a qualitative way, showing both a bi-linear evolution (Fig. 13). The force increases with increasing deflection up to the maximum force reached during puncture (point (1)/(I) up to point (4)/(III)). At point (2)/(II) the slope of the force-deflection curve decreases. This stiffness decrease results from the formation of small cracks on the lower surface of the specimen and is linked to local failure. The reduction in stiffness is more significant for the dynamic loading than for the quasi-static loading rate. The jagged force-deflection evolution for the punctured specimens, loaded in a quasi-static manner, indicates numerous crack formation and growth events at the lower surface of the specimen,

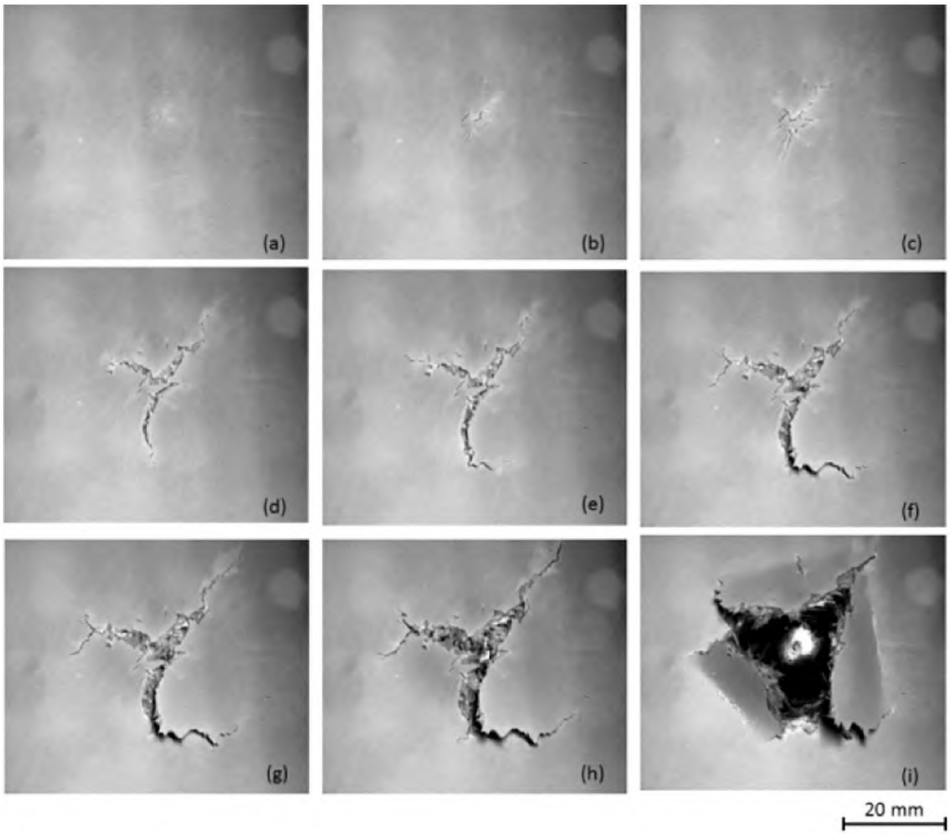

Fig. 8. Damage evolution of punctured glass fiber SMC loaded in a quasi-static manner.

which can clearly be indicated in Fig. 14. During dynamic puncture the specimens also fail due to the formation of a widespread crack network (Fig. 15). For both loading rates the crack network is not as localized as for the glass fiber SMC. After reaching the maximum load, the striker starts penetrating trough the specimen, which still maintains some load until final fracture in point (8)/(V). Then the shaft of the striker slides along the punctured specimen. In this phase, energy is dissipated due to frictional sliding between the specimen and shaft of the striker.

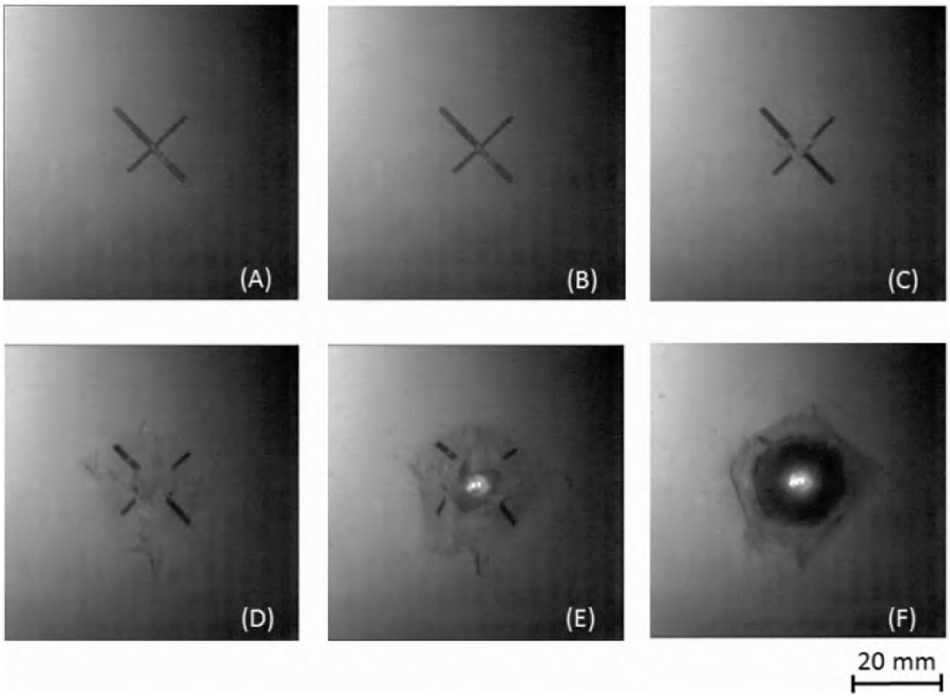

Fig. 9. Damage evolution of punctured glass fiber SMC loaded in a dynamic manner.

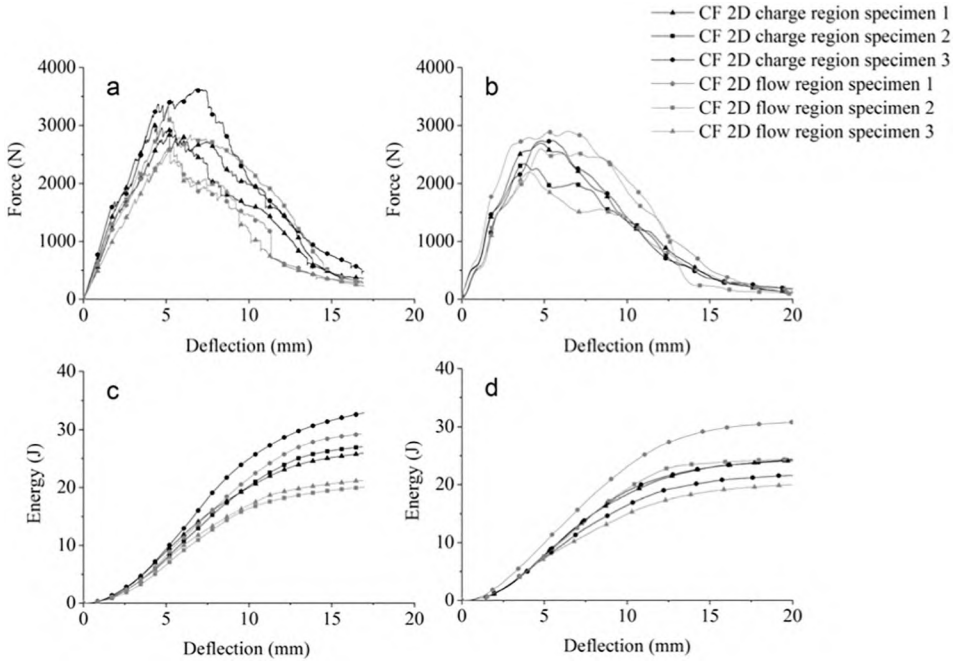

Fig. 10. Quasi-static (a) and dynamic (b) force-deflection and quasi-static (c) and dynamic (d) energy-deflection response resulting from puncture of 2D carbon fiber.

4.4. Post punctured observation of damage region

4.4.1. Micro computed tomography (μCT)

Micro computed tomography enables the investigation of the microstructure of the punctured carbon and glass fiber SMC specimens (Figs. 16 and 17). Although the chosen resolution of the μCT scans does not allow imaging of individual fibers, the microstructure is clearly visible in Fig. 16a and b. The microstructure of the glass fiber SMC can be characterized by 25.4 mm long glass fiber bundles with a diameter of 0.5–1 mm, which was already reported in [19]. The bundles are randomly distributed and oriented in the x-y plane. In contrast, the carbon fiber bundles, which consist of 50,000 individual filaments, tend to spread during manufacturing. This leads to a microstructure which is determined by pseudo-grains or chips with the fibers within one pseudo-grain or chip are oriented in one direction [20,21]. If one takes a closer look inside a punctured carbon fiber specimen, μCT scans clearly show that the damage is not limited to the size of the striker but the cracks propagate further into the material regardless of testing velocity (Fig. 17). The damage induced by the striker propagated into the specimen and led to an asymmetric damage region, which has an elliptical shape with the first principal axes pointing in the fiber direction (Fig. 16c). This indicates that the cracks tend to propagate more easily in flow direction, thus parallel to the reinforcing fibers, than perpendicular to the flow direction for the carbon fiber SMC.

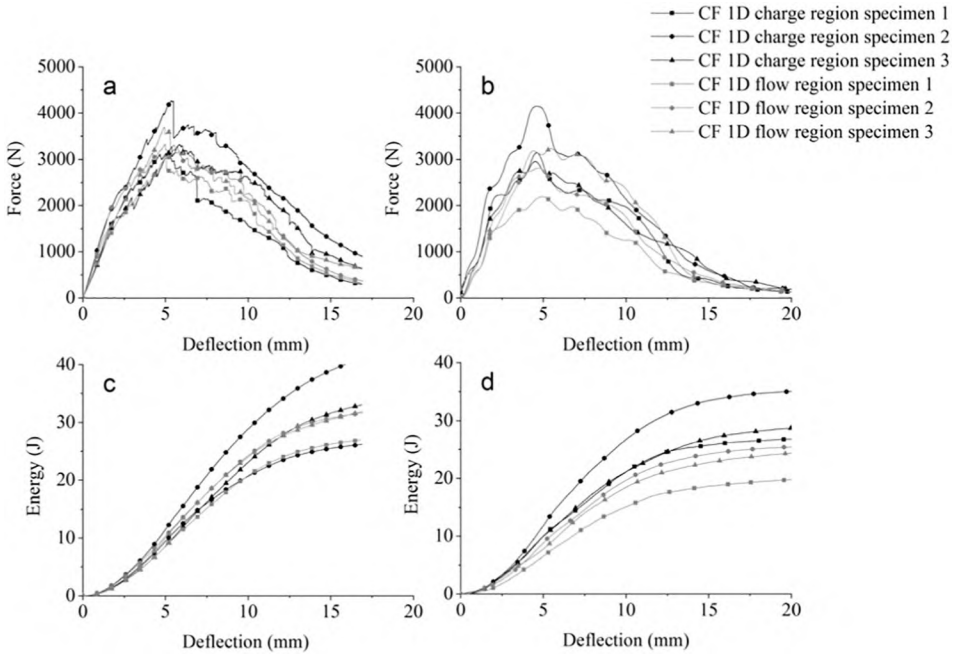

Fig. 11. Quasi-static (a) and dynamic (b) force-deflection and quasi-static (c) and dynamic (d) energy-deflection response resulting from puncture of 1D carbon fiber.

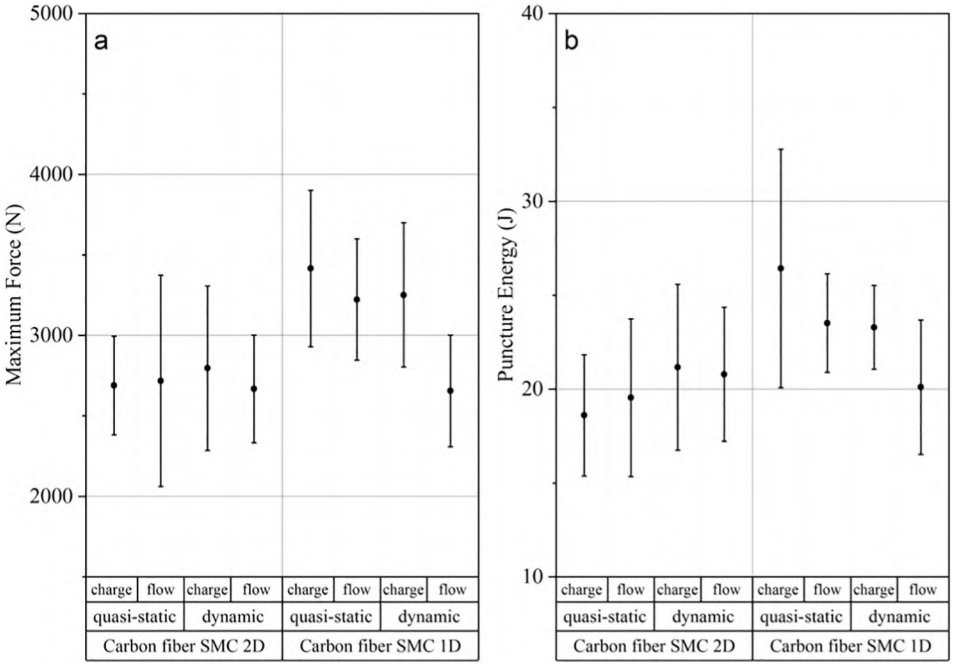

Fig. 12. Maximum unfiltered force and puncture energy for 1D and 2D flow carbon fiber SMC resulting from quasi-static and dynamic puncture.

4.4.2. Scanning electron microscopy (SEM)

Energy absorption of fiber reinforced polymers is based on a number of different failure mechanisms. The failure mechanisms, which could be identified with the aid of scanning electron microscopy (SEM) for glass fiber SMC specimens are interface failure, fiber breakage and matrix failure. For lower loading rates, especially fiber breakage and interface failure between matrix and individual fibers (intra-bundle damage) are present (Fig. 18a).

At higher loading rates, large matrix cracks, which grow perpendicular to the fibers and the interface failure of complete fiber bundles, which can be characterized as pseudo-bundle delamination [22], explain the higher energy absorption capabilities of the glass fiber SMC resulting from a higher loading rate (Fig. 18b). For the carbon fiber SMC (Fig. 18c), damage evolves due to intra-granular and inter-granular failure. Cracks tend to propagate more likely in fiber direction and observations of fractured surface showed inter-fiber fractures which can be described as intra-granular failure due to crack propagation in the carbon fiber pseudo-grains. Pseudo-grain delamination (inter-grain failure) has also to be considered as important failure mechanism. Since the carbon fibers feature an epoxy sizing, the interface between fiber and matrix is rather poor, facilitating the creation of inter-fiber (intra-granular) fractures and inter-granular delamination.

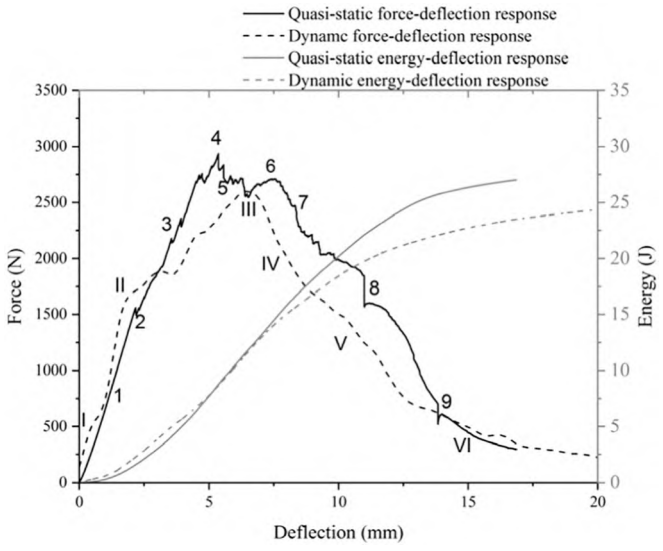

Fig. 13. Force-deflection and energy-deflection responses resulting from quasi-static and dynamic puncture of 2D carbon fiber SMC.

5. Discussion

5.1. Mechanical material and structural properties

With an increase in loading rate, inertia effects have possibly to be considered for impact testing and changes in the force-deflection response may result due to inertia effects rather than due to the material's rate sensitivity. Comparing the findings for the carbon fiber SMC, which show no significant difference in force-deflection response for the two considered loading rates, one can assume that inertia effects can be neglected for this testing series and set up. The low-rate sensitivity of carbon fiber composites has been stated previously in literature. So, if assuming that no rate sensitivity exists due to the comparable force-deflection responses obtained with puncture testing, no significant inertia effects were present when testing at higher loading rates. Taking into account that the glass and carbon fiber SMC specimens have nearly the same thickness and density, thus the specimens feature comparable masses, it can be assumed that inertia effects do also not have to be taken into account for the glass fiber specimens. The maximum strain at failure of both constituents (fibers and matrix) influence energy absorption capability of the composite [23]. Since the two different composites are based on the same resin system, it may be stated that the properties of the fibers as well as the fiber/matrix interface dominate mechanisms for loading rate dependence under puncture loading. However, due to the different fiber volume contents of the two investigated materials the influence of the matrix properties are likely to be different for the glass and carbon fiber SMC. To take this into account, the resulting properties of the two materials cannot be compared directly, but each material has to be considered and evaluated at its own.

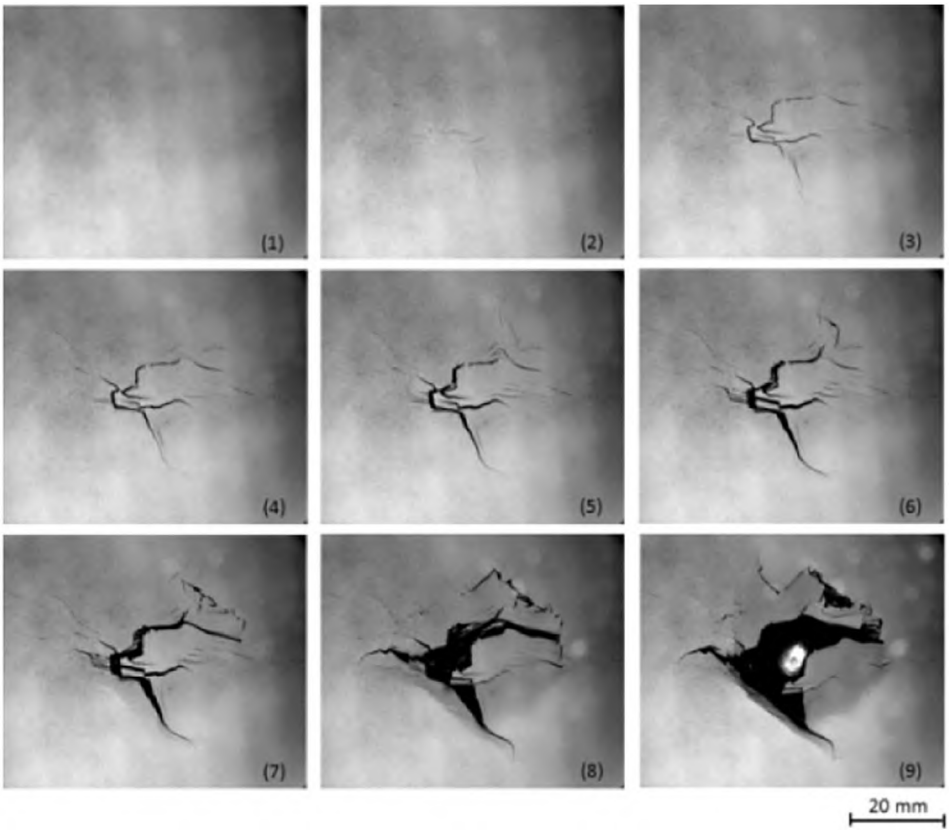

Fig. 14. Damage evolution punctured carbon fiber SMC loaded in a quasi-static manner.

The increase of maximum force for higher loading rates observed for the glass fiber SMC specimens could be explained by an increase of tensile strength of glass fibers as shown by Arao et al. [24]. An increase in tensile strength of glass fiber SMC with higher loading rates was also reported by Shirinbayan et al. [22].

Carbon fiber SMC was noted to be insensitive to loading rate in the investigated range, showing only a slight trend to negative loading rate sensitivity for highly anisotropic plaques. The rate independence of unidirectional carbon fiber reinforced polymers was already shown by Harding and Welsh [25]. This study generally reflects the non-rate

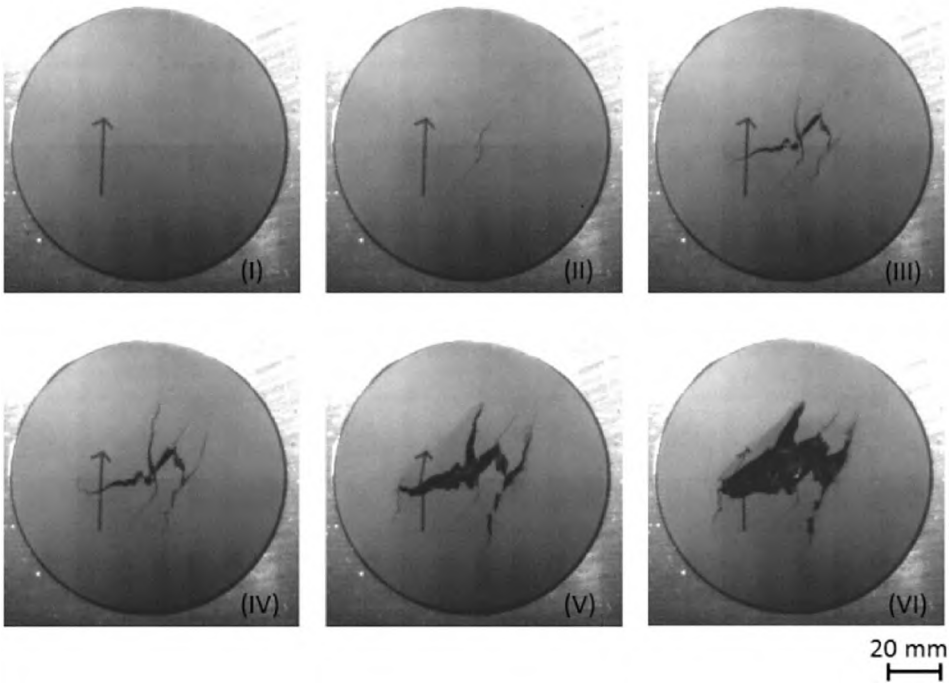

Fig. 15. Damage evolution of carbon fiber SMC loaded in a dynamic manner.

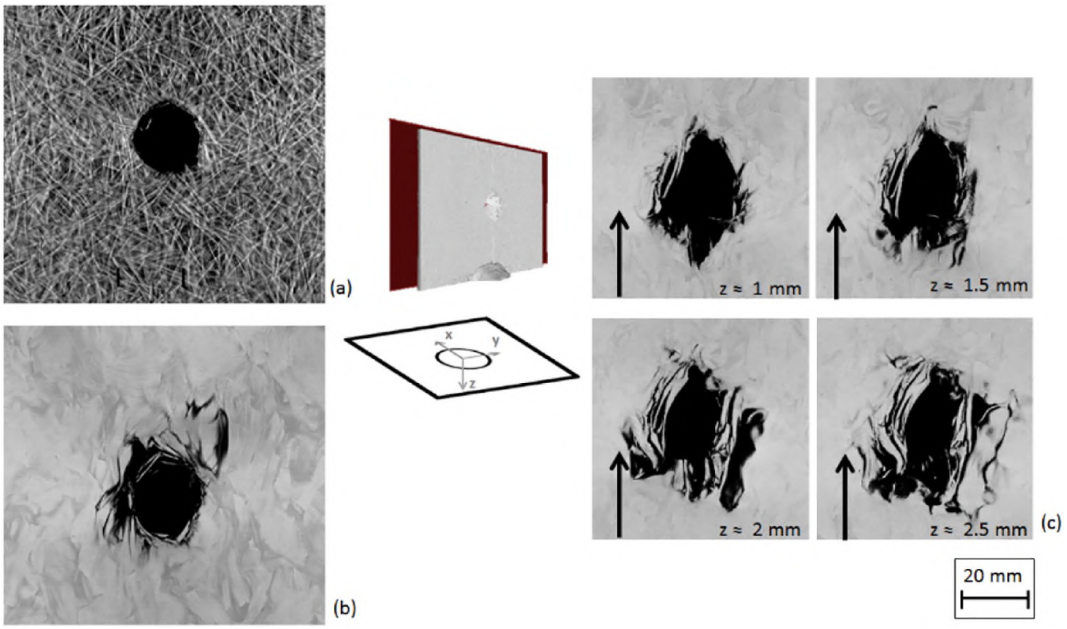

Fig. 16. μCT images of punctured glass (a) and carbon (b and c) fiber SMC specimen, with z equal to zero at the top surface of the specimen and the arrow indicating flow direction.

sensitivity of carbon fibers and this finding can be transferred to the results of this study.

The heterogeneity of the microstructure of the investigated carbon fiber SMC, which is determined by pseudo-grains also explains the significant scatter of tensile and puncture properties.

5.2. Damage evolution and failure

The failure mechanisms of the two SMC materials are significantly influenced by the microstructure. Damage evolution of the glass fiber SMC specimens is dominated by interface failure and matrix cracking. This contradicts with the results of Kau who identified mainly fiber pull-out and fiber breakage as failure mechanisms in punctured glass fiber SMC loaded in a dynamic way [7]. The changing failure mechanisms from individual fiber-matrix interface failure to the interface failure of entire fiber bundles (pseudo-bundle delamination) linked to large matrix cracks, explains the capabilities of glass fiber SMC to absorb more energy for higher loading rates. It can be concluded that the mechanical behavior of the interface and interface strength is possibly rate dependent.

For the carbon fiber SMC, it is assumed that the locally highly orientated fibers strongly to affect penetration behavior and damage.

Consistent to the findings reported by Chaturvedi et al. [26], the shape of the damaged region of punctured SMC specimen was observed not to be regular. This irregular shape results from inhomogeneity of the material due to the non-uniform distribution of the fibers, especially for the 1D flow carbon fiber plaques. Especially the carbon fiber SMC exposed to puncture loading was extremely sensitive to the formation of inter-fiber cracks (intra-granular failure). Pseudo-grain delamination (inter-granular failure) also increased the size of the punctured region due to a failure at pseudo-grain boundaries.

6. Conclusion

A 2D flow during compression molding of the semi-finished sheets does not influence tensile properties of glass and carbon fiber SMC, however, mechanical properties of flow region specimens show a

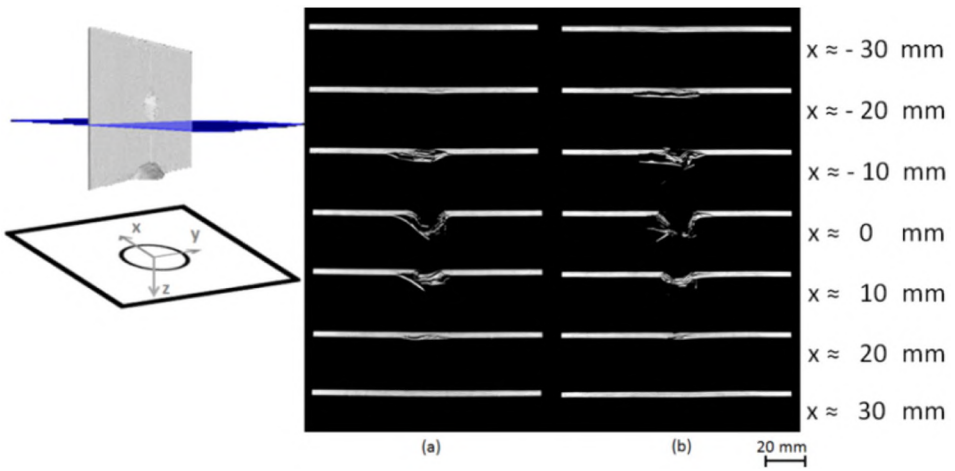

Fig. 17. μCT images of punctured carbon fiber SMC punctured in a quasi-static (a) and dynamic (b) manner at different positions along x-axis. X is equal to zero at the center of the specimen.

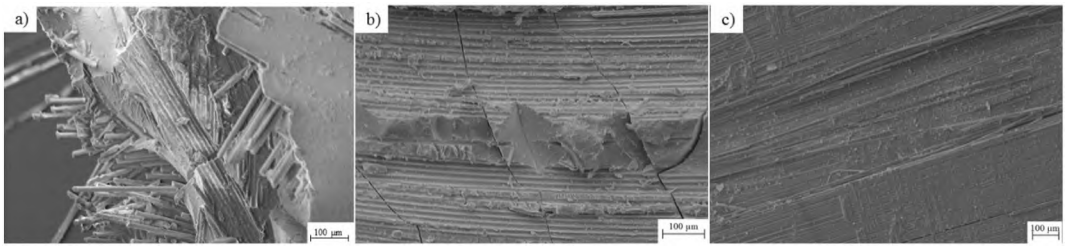

Fig. 18. Scanning electron microscopy of fractured surface of punctured glass fiber SMC loaded in a quasi-static (a) and dynamic manner (b) and fractured surface of punctured carbon fiber SMC loaded in a dynamic manner (c).

slightly higher scatter. 1D flow of semi-finished carbon fiber sheets leads to anisotropic mechanical properties. The investigated glass fiber SMC illustrated a positive loading rate dependence with a significant increase of maximum force (65% for charge region specimens and 73% for flow region specimens) and puncture energy (67% for charge region specimens and 64% for flow region specimens). In contrast, the investigated carbon fiber SMC was observed to be insensitive to a variation of loading rate associated with the loading rates/configurations investigated within this study when strength and absorbed energy are considered.

The SMC specimens, independent of type of reinforcement, showed similar damage evolution, involving multiple crack initiation and growth. The formation of cracks was more localized for glass fiber SMC, thus the cracks propagate more easily trough the carbon fiber SMC. For the glass fiber SMC, large matrix cracks and interface failure between matrix and complete fiber bundles (pseudo-delamination) enhance energy absorption capabilities at higher loading rates. Matrix and interface properties play an important role for evolving damage. The microstructure of the carbon fiber SMC is dominated by pseudo-grains with all fibers inside a pseudo-grain oriented in the same direction. Exposed to tensile or puncture loading, carbon fiber SMC mainly fails due to inter-fiber (intra-granular) fractures. Pseudo-grain delamination (inter-granular failure) is another important damage mechanisms resulting from puncture and tensile loading. Thus, material properties and damage are mainly influences by the pseudo-grain like microstructure and the locally highly oriented carbon fibers. In general, the damage region of punctured carbon fiber SMC specimens, which experienced quasi-static or dynamic loading, is larger than the diameter of the penetrating striker and has an irregular shape, following the local fiber orientation.

Acknowledgements

The research documented in this manuscript has been funded by the German Research Foundation (DFG) within the International Research Training Group “Integrated engineering of continuous-discontinuous long fiber reinforced polymer structures” (GRK 2078). The support by the German Research Foundation (DFG) as well as the Ontario Research Foundation (ORF) and the Natural Science and Engineering Research Council of Canada (NSERC) is gratefully acknowledged. The authors also kindly acknowledge the Fraunhofer ICT in Pfinztal, Germany for manufacturing the SMC with a special thanks to D. Bücheler.

Data availability

The raw/processed data required to reproduce these findings cannot be shared at this time as the data also forms part of an ongoing study.

References

[1] M. Bruderick, D. Denton, M. Shinedling, M. Kiesel, Application of carbon fiber SMC for the dodge viper, http://www.quantumcomposites.com/pdf/papers/Viper-SPE-Paper.pdf, Accessed date: 24 January 2018.
[2] U. Reimer, G. Esswein, H. Derek, Quo Vadis - SMC im Automobilbau, KU Kunststoffe Online-Archiv 90 (2000) 86–90.
[3] G. Gardiner, Is the BMW 7 Series the future of autocomposites? http://www.compositesworld.com/articles/is-the-bmw-7-series-the-future-of-autocomposites 2016, Accessed date: 24 January 2018.
[4] G. Lamanna, A. Ceprano, Mechanical characterization of sheet moulding composites for the automotive industry, TOMSJ 8 (2014) 108–113, https://doi.org/10.2174/1874088X01408010108.
[5] M. Oldenbo, S.P. Fernberg, L.A. Berglund, Mechanical behaviour of 5SMC6 composites with toughening and low density additives, Compos. A: Appl. Sci. Manuf. 34 (2003) 875–885, https://doi.org/10.1016/S1359-835X(03)00155-6.
[6] S. Boylan, J.M. Castro, Effect of reinforcement type and length on physical properties, surface quality, and cycle time for sheet molding compound (SMC) compression molded parts, J. Appl. Polym. Sci. 90 (2003) 2557–2571, https://doi.org/10.1002/app.12726.
[7] H.T. Kau, A study of the impact behavior of chopped fiber reinforced composite, Polym. Compos. 11 (1990) 253–264, https://doi.org/10.1002/pc.750110502.
[8] B. Sadasivam, P.K. Mallick, Impact damage resistance of random fiber reinforced automotive composites, J. Thermoplast. Compos. Mater. 15 (2002) 181–191, https://doi.org/10.1177/0892705702015003438.
[9] S.-M. Lee, J.-S. Cheon, Y.-T. Im, Experimental and numerical study of the impact behavior of SMC plates, Tenth International Conference on Composite Structures, 47, 1999, pp. 551–561, https://doi.org/10.1016/S0263-8223(00)00021-0.
[10] J.P. Dear, S.A. Brown, Impact damage processes in reinforced polymeric materials, Compos. A: Appl. Sci. Manuf. 34 (2003) 411–420, https://doi.org/10.1016/S1359-835X(03)00082-4.
[11] S.K. Chaturvedi, R.L. Sierakowski, Effects of impactor size on impact damage-growth and residual properties in an SMC-R50 composite, J. Compos. Mater. 19 (1985) 100–113, https://doi.org/10.1177/002199838501900201.
[12] D. Bücheler, Locally continuous-fiber reinforced sheet molding compound. Dissertation, Karlsruhe Institute of Technology, https://publikationen.bibliothek.kit.edu/1000079163,2018, Accessed date: 23 January 2018.
[13] M. Fette, M. Hentschel, J.G. Santafe, T. Wille, H. Büttemeyer, P. Schiebel, New Methods for Computing and Developing Hybrid Sheet Molding Compound Structures for Aviation Industry, 1st CIRP Conference on Composite Materials Parts Manufacturing (CIRP CCMPM 2017), 66, 2017 45–50, https://doi.org/10.1016/j.procir.2017.03.289.
[14] M. Fette, M. Hentschel, F. Köhler, J. Wulfsberg, A. Herrmann, Automated and Cost-efficient Production of Hybrid Sheet Moulding Compound Aircraft Components, 16th Machining Innovations Conference for Aerospace Industry - MIC 2016, 6, 2016 132–139, https://doi.org/10.1016/j.promfg.2016.11.017.
[15] M. Fette, M. Reiß, J. Wulfsberg, N. Stoess, M. Hentschel, New approach for the efficient manufacturing of sandwich structures based on sheet moulding compounds, Adv. Mater. Res. (2016) 264–271, https://doi.org/10.4028/www.scientific.net/AMR.1140.264.
[16] J. Wulfsberg, A. Herrmann, G. Ziegmann, G. Lonsdorfer, N. Stöß, M. Fette, Combination of carbon fibre sheet moulding compound and prepreg compression moulding in aerospace industry, Procedia Eng. 81 (2014) 1601–1607, https://doi.org/10.1016/j.proeng.2014.10.197.
[17] D.M. Corbridge, L.T. Harper, D.S.A. de Focatiis, N.A. Warrior, Compression moulding of composites with hybrid fibre architectures, Compos. A: Appl. Sci. Manuf. 95 (2017) 87–99, https://doi.org/10.1016/j.compositesa.2016.12.018.
[18] F. Gortner, L. Medina, P. Mitschang, Influence of textile reinforcement on bending properties and impact strength of SMC-components, Int. J. Appl. Sci. Technol. 8 (2015) 259–269.
[19] P. Dumont, L. Orgéas, D. Favier, P. Pizette, C. Venet, Compression moulding of SMC. In situ experiments, modelling and simulation, Compos. A: Appl. Sci. Manuf. 38 (2007) 353–368, https://doi.org/10.1016/j.compositesa.2006.03.010.
[20] H. Xu, Modeling and simulation of compression molding process for sheet molding compound (SMC) of chopped carbon fiber composites, SAE Int. J. Mater. Manuf. 10 (2017)https://doi.org/10.4271/2017-01-0228.
[21] Z. Chen, Y. Li, Y. Shao, T. Huang, H. Xu, Y. Li, W. Chen, D. Zeng, K. Avery, H. Kang, X. Su, A Comparative Study of Two RVE Modelling Methods for Chopped Carbon Fiber SMC, 2017https://doi.org/10.4271/2017-01-0224.
[22] M. Shirinbayan, J. Fitoussi, F. Meraghni, B. Surowiec, M. Bocquet, A. Tcharkhtchi, High strain rate visco-damageable behavior of advanced sheet molding compound (A-SMC) under tension, Compos. Part B 82 (2015) 30–41, https://doi.org/10.1016/j.compositesb.2015.07.010.

[23] G.L. Farley, Effect of fiber and matrix maximum strain on the energy absorption of composite materials, J. Compos. Mater. 20 (1986) 322–334, https://doi.org/10.1177/002199838602000401.
[24] Y. Arao, N. Taniguchi, T. Nishiwaki, N. Hirayama, H. Kawada, Strain-rate dependence of the tensile strength of glass fibers, J. Mater. Sci. 47 (2012) 4895–4903, https://doi.org/10.1007/s10853-012-6360-z.
[25] J. Harding, L.M. Welsh, A tensile testing technique for fibre-reinforced composites at impact rates of strain, J. Mater. Sci. 18 (1983) 1810–1826, https://doi.org/10.1007/BF00542078.
[26] S.K. Chaturvedi, R.L. Sierakowski, Residual strength assessment of SMC composites subjected to dynamic impact, Compos. Struct. 1 (1983) 137–161, https://doi.org/10.1016/0263-8223(83)90009-0.